



Alexandria University
Alexandria Engineering Journal

www.elsevier.com/locate/aej
www.sciencedirect.com



Carrier frequency offset estimation for MIMO single-carrier FDMA system in wireless communication



Ehab F. Badran ^{a,*}, Marwa Samara ^b, Nour Eldin Ismail ^c

^a Department of Electronics and Communications Engineering, College of Engineering and Technology, Arab Academy for Science, Technology and Maritime Transport, Alexandria 21937, Egypt

^b Department of Electrical Engineering, Alexandria Higher Institute of Engineering & Technology (AIET), Alexandria 21311, Egypt

^c Department of Electrical Engineering, Alexandria University, Alexandria 21544, Egypt

Received 23 September 2021; revised 9 December 2021; accepted 15 December 2021

Available online 29 December 2021

KEYWORDS

CAZAC sequence;
 Barker code;
 Frequency offset compensation;
 MIMO SC-FDMA

Abstract Multiple-Input Multiple-Output (MIMO) Orthogonal Frequency-Division Multiplexing (OFDM) systems and Single-Carrier Frequency-Division Multiple Access (SC-FDMA) are so susceptible to carrier frequency offset (CFO) between transceivers. In this paper, a novel sequence called CAZBAR is proposed. The proposed CAZBAR sequence is based on constant amplitude zero autocorrelation (CAZAC) sequence and barker code. CAZBAR sequence shows better autocorrelation with higher peak at zero shift without ripples, which facilitates estimating carrier frequency offset in communication systems compared to other compensation methods in terms of mean square error (MSE). By applying CAZBAR sequence in MIMO SC-FDMA system 2×2 and 4×4 , the bit error rate (BER) performance has improved significantly. At a BER = 10^{-2} , a SNR reduction of 11 dB is achieved for 2×2 system and 7 dB reduction for 4×4 system compared to other sequences. Which improves the performance of the whole system MIMO SC-FDMA. The CAZBAR sequence can be applied in 5G techniques, MIMO-OFDM, and MIMO SC-FDMA systems.

© 2021 THE AUTHORS. Published by Elsevier BV on behalf of Faculty of Engineering, Alexandria University. This is an open access article under the CC BY-NC-ND license (<http://creativecommons.org/licenses/by-nc-nd/4.0/>).

1. Introduction

Nowadays, orthogonal frequency-division multiple-access (OFDMA) act as multi-carrier multi-user transmission tech-

nology used in different wireless communication systems. There are two main drawbacks in implementing OFDMA systems [1]. First, need high power to send data cause high peak-to-average-power ratio (PAPR) and second, mismatch between carrier frequencies leads to carrier frequency offsets (CFOs). High PAPR leads to the amplifier of transmitter works with high power that cause decrease in the energy efficiency of the system. Thus, PAPR reduction techniques [2–5], and the references therein, have to be utilized in

* Corresponding author.

E-mail address: ebadran@aast.edu (E.F. Badran).

Peer review under responsibility of Faculty of Engineering, Alexandria University.

<https://doi.org/10.1016/j.aej.2021.12.036>

1110-0168 © 2021 THE AUTHORS. Published by Elsevier BV on behalf of Faculty of Engineering, Alexandria University. This is an open access article under the CC BY-NC-ND license (<http://creativecommons.org/licenses/by-nc-nd/4.0/>).

OFDMA system. Energy efficiency is a critical issue in transmissions for mobile users (MUs)'s battery. Due to its lower PAPR, single-carrier frequency-division multiple-access (SC-FDMA) has been widely used. SC-FDMA is currently common in uplink of Long-Term Evolution (LTE). It prevents distorting the signal, designing simple transceiver system and consuming low power and this leads to expansion battery life of mobile phones. In [6], a space frequency block codes MIMO single-carrier code frequency- division multiple access (SFBC MIMO SC-CFDMA) transceiver was proposed to improve the BER performance over the traditional SFBC SC-FDMA system. As to OFDM system, also SC-FDMA is critical to carrier frequency offset (CFO) [7]. It occurs due to mismatching between transmitter and receiver causing doppler shift. CFO causes disturbance of orthogonality between subcarriers, thus reduce the performance of the system dramatically. In transmission data, multiple users are sending multiple signals through multiple antenna [8] where affected by various values of CFO. After passing through channels, at the receiver the signals are collected again. This collection leads to Multiple Access Interference (MAI). For an effective system, efficient CFO synchronization is essential. The normalized CFO is broken into two parts: integral CFO (IFO) ε_i as well as fractional CFO (FFO) ε_f . IFO causes a cyclic shift to the appropriate subcarrier on the receiver side. The orthogonality of the sub-carrier frequency components is not destroyed by IFO. FFO, on the other hand, breaks the orthogonality between the sub-carriers.

To get efficient CFO synchronization, there are a lot of preamble-based timing strategies have been studied.

Mainly there are two types of strategies. The first one depends on data aided strategy. In this strategy, transmitting the preamble and to reach synchronization depends on autocorrelation or cross correlation of received signal. Also, one of the benefits of correlation products is to improve the estimation of time metric. The second strategy is non-aided method also known as blind synchronization [8]. Synchronization is reached by applying statistical properties on the received signal. From its drawback it needs large estimator mean square error (MSE) to deal with complex computational algorithms. The novel proposed sequence is used as data aided schemes so the system performance more efficiency with less overhead.

In this paper, focuses on FFO to avoid destroying orthogonality between the sub-carriers, besides synchronization method based on data aided scheme is considered. A sequence called CAZBAR which is based on both of CAZAC sequence and barker code, takes the benefits of both, is proposed. CAZBAR sequence can be used in CFO estimation in different multicarrier systems such as OFDM, SCFDMA, and MIMO SC-FDMA. Simulation results shows that the proposed CAZBAR sequence gives good improving in BER performance, and it is better in indicating the start of the frame with a sharper peak of the autocorrelation function than other sequences.

The paper is organized as follows; section 2 explains the formation process of the proposed CAZBAR sequence and its great effect in CFO estimation methods. In section 3, the proposed MIMO SC-FDMA model is described. BER analysis of the proposed model is presented. Section 5 presents the computational complexity of the system. In section 6 simulation results are discussed. Finally, in Section 7, conclusions are observed.

2. Formation of CAZBAR sequence

The proposed CAZBAR sequence is based on both of CAZAC and barker code. CAZAC sequence is a phase shift pulse code which is well known with zero periodic correlation except peak for zero shift. Barker code, with is known by its ideal autocorrelation property, is a finite sequence of digital values. By multiplying CAZAC sequence with a repeated version of a specific length of Barker codes, the proposed CAZBAR sequence is generated. CAZBAR sequence has a better correlation property than CAZAC sequence. It can be used in different application as radar systems or for a method of synchronization and carrier frequency estimation in communication systems. The CAZAC sequence is formed using equation (1) with L is the length of CAZAC sequence and a is a prime number.

$$c(l) = e^{j\left(\frac{\pi a l^2}{L}\right)}, l = 0, 1, \dots, L - 1, \quad (1)$$

Then the output from multiplying CAZAC with barker, convert it in frequency domain by passing through FFT to be suitable for OFDM system. The proposed sequence is composed of two halves, the first one (**A**) is CAZBAR codes, while second one (**B**) is the flipped complex conjugate of **A**. At receiver side, correlation function is applied between the received signal and the local sequence to detect the peak of time synchronization. A list of Barker codes with different lengths is shown in Table 1.

The next Fig. 1-a to 1-h show the autocorrelation of CAZAC sequence and autocorrelation of proposed CAZBAR sequence with different barker lengths. As shown from figures, CAZBAR code with length 4 and 2 represent better performance compared with CAZAC. as by length 2 the next maximum value is 0.04953 and by length 4 the next maximum value is 0.04896. while in CAZAC the next maximum value in 0.1151.

In Fig. 2, a comparison of the BER performance of MIMO SC-FDMA system using CAZBAR with different lengths of Barker code is illustrated. As shown from Fig. 2, the BER performance has a slight difference response when change in barker lengths L . At $BER = 10^{-4}$ the SNR reaches 7.80 dB by CAZBAR sequence with Barker length $L = 2$, and reaches 8.1 dB by using $L = 7$ and 13 as there is no different between them.

Therefore, thought out this paper, a CAZBAR sequence that is based on Barker code of length 2 will be considered.

Table 1 List of barker codes.

Length	Codes	Sidelobe level
2	+1-1 or + 1 + 1	-6dB
3	+1 + 1-1	-9.5 dB
4	+1 + 1-1 + 1 or + 1 + 1 + 1-1	-12 dB
5	+1 + 1 + 1-1 + 1	-14 dB
7	+1 + 1 + 1-1-1 + 1-1	-16.9 dB
11	+1 + 1 + 1-1-1-1 + 1-1-1 + 1-1	-20.8 dB
13	+1 + 1 + 1 + 1 + 1-1-1 + 1 + 1-1	-22.3 dB
	1 + 1-1 + 1	

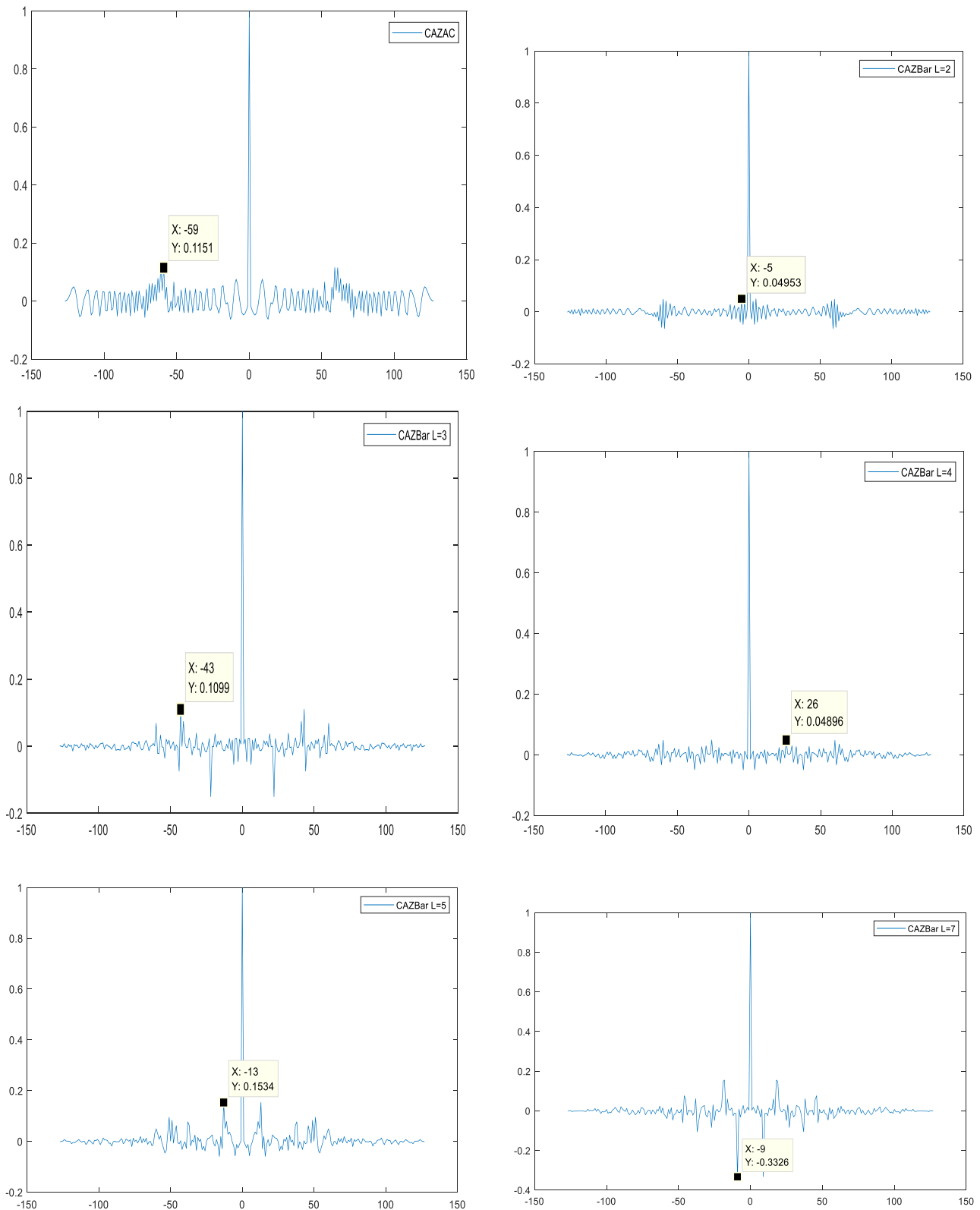


Fig. 1 The autocorrelation of CAZAC sequence and proposed CAZBAR sequence with different barker lengths.

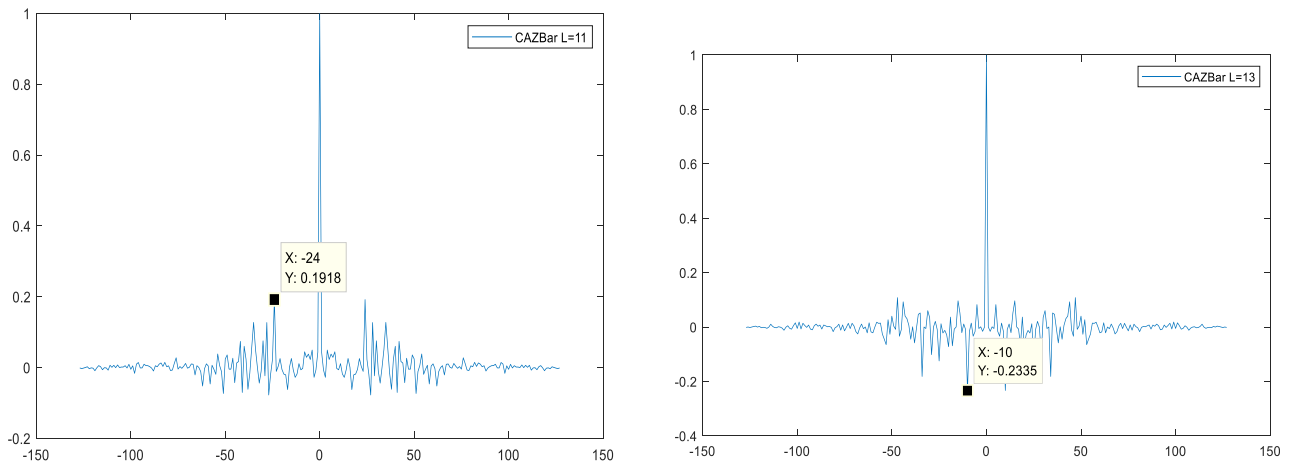
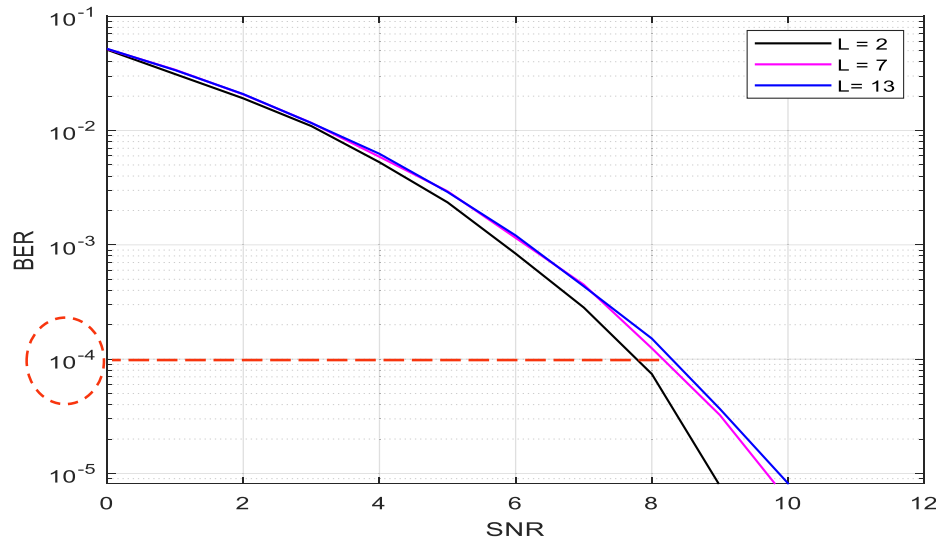


Fig. 1 (continued)

Fig. 2 BER of MIMO SC-FDMA using CAZBar with different barker length $L = 2, 7, 13$.

3. The proposed MIMO SC-FDMA system model

A. MIMO-SC-FDMA Transmitter

The k^{th} user sends data symbols vector \mathbf{d}^k which is spatially demultiplexed into P vectors $\{\mathbf{d}_p^k\}_{p=1}^P$ each of length N , where \mathbf{d}_p^k is the k^{th} user data symbols in the p^{th} antenna branch [9]. N -point FFT is applied to each vector \mathbf{d}_p^k to form \mathbf{D}_p^k the frequency domain symbols of the k^{th} user data symbols in the p^{th} antenna branch, which can be expressed as

$$\mathbf{D}_p^k = \mathbf{F}_N \mathbf{d}_p^k, \quad (2)$$

The proposed MIMO-SC-FDMA system is shown in Fig. 3.

where \mathbf{F}_N is $N \times N$ isometric FFT matrix, \mathbf{D}_p^k vector is then subcarrier mapped into $M \times 1$ vector, $M = QN$, Q is the bandwidth expansion factor and the maximum number of users in the transmission. The M -IFFT process transform the output of subcarrier mapping from frequency

domain to time domain. For subcarrier mapping there are two main methods:

- localized mapping (LFDMA), the outputs of Fast Fourier transform (FFT) are mapped. Then the number of sub-carriers is allocated in one contiguous block for each user.
- Interleaved (distributed) mapping (IFDMA), the outputs of FFT are mapped. then sub-carriers are disturbed over the whole bandwidth [10].

The IFDMA method shows a low peak to-average ratio (PAPR), but very sensitivity to CFOs as in OFDMA system. While the LFDMA method is more powerful against multiple access interference (MAI), but it leads to high PAPR compared to the IFDMA method.

After mapping the signal pass through IFFT block which converts signal to time domain with mathematical expression is s_k . The isometric matrix of M -point FFT \mathbf{F}_N has entries $F_N^{n,k} = \frac{1}{\sqrt{N}} e^{-j\frac{2\pi nk}{N}}$ with $n, k \in \{0, 1, 2, \dots, N-1\}$ is defined as

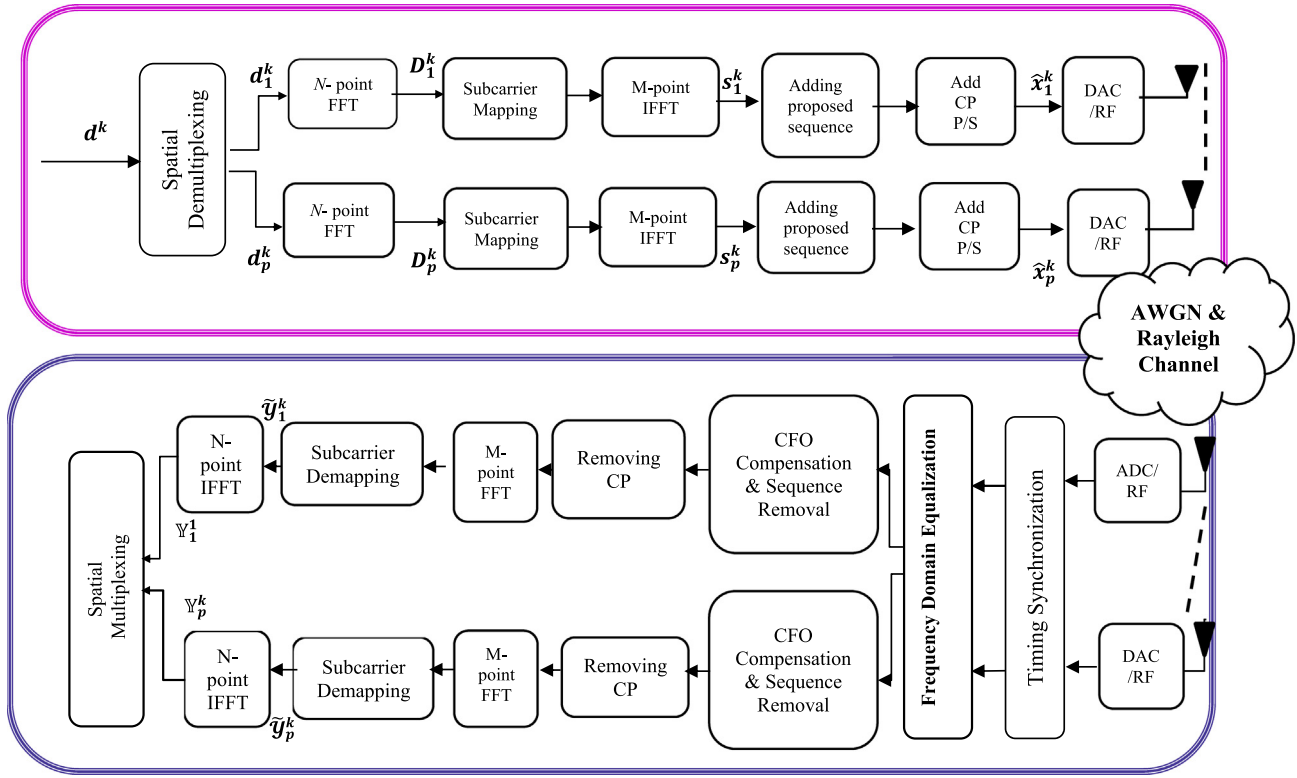


Fig. 3 Block Diagram of MIMO-Single-carrier FDMA system.

$$\mathbf{F}_N = \begin{pmatrix} F_N^{0,0} & F_N^{0,1} & \dots & F_N^{0,(N-1)} \\ F_N^{1,0} & F_N^{1,1} & \dots & F_N^{1,(N-1)} \\ \vdots & \vdots & \ddots & \vdots \\ F_N^{(N-1),0} & F_N^{(N-1),1} & \dots & F_N^{(N-1),(N-1)} \end{pmatrix}. \quad (3)$$

The \mathbf{F}_M^H is matrix of an IFFT with size $M \times M$. \mathbf{M}_k is $M \times N$ the matrix of subcarrier mapping for the k^{th} user.

$$\mathbf{s}_p^k = \mathbf{F}_M^H \mathbf{M}_k \mathbf{D}_p^k \quad (4)$$

The subcarrier mapping matrix \mathbf{M}_k for the interleaved mapping (IM) and localized mapping (LM) schemes can be expressed as [11]

$$\mathbf{M}_k = \begin{cases} [0_{(k-1) \times N}; k_1^T; 0_{(Q-1) \times N}; k_2^T; \dots; k_N^T; 0_{(Q-k) \times N}] \text{IM}, & (5a) \\ [0_{(k-1)N \times N}; \mathbf{I}_N; 0_{(M-kN) \times N}] \text{LM} & (5b) \end{cases} \quad (5)$$

The proposed CAZBAR sequence of length L_q is passing through two steps separately before adding to MIMO SC-FDMA system: first is mapped either by localized or interleaved mapping, second converted in time domain. Then proposed sequence is ready to be added after IFFT block. which improve estimation of carrier frequency offset takes place after the IFFT process to form the vector x_k of length as

$$\mathbf{x}_p^k = \begin{bmatrix} \mathbf{s}_p^k & \mathbf{q}_k^T \end{bmatrix}^T. \quad (6)$$

Then, the L_c cyclic prefix is added to x_k . Therefore, the signal \hat{x}_k with C_p is cyclic prefix of size $(M + L_q + L_c) \times 2M$, q_k is the proposed used sequence with length L_q can be expressed as

$$\hat{\mathbf{x}}_p^k = C_p \mathbf{x}_p^k, \quad (7)$$

B. MIMO-SC-FDMA Receiver

Then signals $\{\hat{\mathbf{x}}_p^k\}_{p=1}^P$ are transmitted passing through channel, which is Rayleigh fading channel [12]. The channel is a frequency-selective fading channel and each user experiences a different channel impulse response. Based on the assumption that all K users are synchronized in time.

where

- \mathcal{Y}_j is received signal vector of length $(M + L_q) \times 1$ in the j^{th} receive antenna branch.
- H_{ji}^k is multipath channel circulant matrix between i^{th} transmitter antenna and j^{th} received antenna.
- \mathcal{W}_{ji}^k is a CFOs matrix that shows as diagonal the of the k^{th} user, where $\mathcal{W}_{ji}^k = e^{j2\pi m \epsilon_{ji}^k / M}$.
- ϵ_{ji}^k is the normalized CFO of the k^{th} user.
- n_j is complex Gaussian noise vector.

So the received signals are affected by carrier frequency offset derived as

$$\mathcal{Y}_j = \sum_{k=1}^K \sum_{i=1}^P \mathcal{W}_{ji}^k H_{ji}^k \mathbf{x}_i^k + n_j, \quad (8)$$

The joint MIMO equalization process with carrier frequency offset is formed on received signal \mathcal{Y}_j . In this paper, minimum mean square error (MMSE) is used on proposed system, the equalizer weight matrix E_{ji}^k is formed as [13]

$$\mathbf{E}_j^k = \begin{bmatrix} \mathbf{E}_{11}^k & \mathbf{E}_{12}^k & \cdots & \mathbf{E}_{1N_r}^k \\ \mathbf{E}_{21}^k & \mathbf{E}_{22}^k & \cdots & \mathbf{E}_{2N_r}^k \\ \vdots & \vdots & \ddots & \vdots \\ \mathbf{E}_{N_r1}^k & \mathbf{E}_{N_r2}^k & \cdots & \mathbf{E}_{N_rN_r}^k \end{bmatrix} = \begin{cases} \left\{ \mathbf{H}^{k^H} \mathbf{H}^k \right\}^{-1} \mathbf{H}^{k^H}, ZF \\ \left\{ \mathbf{H}^{k^H} \mathbf{H}^k + \frac{1}{\text{SNR}} \mathbf{I}_{2N_r} \right\}^{-1} \mathbf{H}^{k^H}, MMSE \end{cases} \quad (9)$$

where \mathbf{H}^k is effective frequency domain channel matrix, can be expressed as

$$\mathbf{H}^k = \begin{bmatrix} \mathbf{H}_{11}^k & \mathbf{H}_{12}^k & \cdots & \mathbf{H}_{1N_r}^k \\ \mathbf{H}_{21}^k & \mathbf{H}_{22}^k & \cdots & \mathbf{H}_{2N_r}^k \\ \vdots & \vdots & \ddots & \vdots \\ \mathbf{H}_{N_r1}^k & \mathbf{H}_{N_r2}^k & \cdots & \mathbf{H}_{N_rN_r}^k \end{bmatrix} \quad (10)$$

Next step making CFO estimation as CFO can disturb the orthogonality between sub-carriers which effects the performance of SC-FDMA. Inter Carrier Interference ICI arises due to frequency offset.

Different methods are discussed to illuminate effects of CFO

- Schmidl and Cox [14] method depends on combining two identical parts of PN sequence each of length $N/2$.
- Minn's Method [15–17] the sequence is based on four parts each part with length $N/4$. Where the first two parts are identical PN sequence and the other two are the negative sign of first two.
- Constant Amplitude Zero Autocorrelation (CAZAC sequence) related to R. Frank, S. Zadoff [18–20].
- CAZBAR sequence based on barker multiplied with CAZAC sequence as shown previous.

This combination has a good cross-correlation and auto-correlation functions in time domain form. Correlation equation is given by

$$P_j(m) = \sum_{n=0}^{\frac{N}{2}-1} \mathcal{Y}_j(m-n) \mathcal{Y}_j(m+n+1), m=0, 1, \dots, N-1 \quad (11)$$

The timing synchronization estimator is $R_j(m)$, $\widehat{\mathcal{Y}}_j$ is equalized received signal, N number of subcarriers, and where n is the index of the sample, equivalent to the subcarrier index.

$$R_j(m) = \frac{1}{2} \sum_{n=0}^{\frac{N}{2}-1} \left| \mathcal{Y}_j \left(m+n-\frac{N}{2} \right) \right|^2, \quad (12)$$

The timing metric τ_j is computed using $P(m)$ divided by $R(m)$ as given in (9).

$$\tau_j = \arg \max \left(\frac{|P_j(m)|^2}{(R_j(m))^2} \right). \quad (13)$$

The CFO ε_j at the j^{th} receive antenna can be expressed as

$$\varepsilon_j = \text{angle} \frac{P_j(\tau_j)}{2\pi}. \quad (14)$$

The received signal \mathcal{Y}_j after CFO compensation is

$$\mathcal{Y}_j = \begin{bmatrix} \gamma_{11}^k & \gamma_{12}^k & \cdots & \gamma_{1N_r}^k \\ \gamma_{21}^k & \gamma_{22}^k & \cdots & \gamma_{2N_r}^k \\ \vdots & \vdots & \ddots & \vdots \\ \gamma_{N_r1}^k & \gamma_{N_r2}^k & \cdots & \gamma_{N_rN_r}^k \end{bmatrix} \mathcal{Y}_j, \quad (15)$$

After that remove the proposed sequence and cyclic prefix, the received signal pass through \mathbf{F}_N^H is the matrix of IFFT with size $N \times N$ forming \mathcal{Y}_j , then \mathbf{M}_k^T is $M \times N$ the matrix of sub-carrier demapping for the k^{th} user, finally \mathbf{F}_M is $M \times M$ FFT matrix to get the desired data.

$$\mathbf{y}_j^k = \mathbf{F}_N^H \mathbf{M}_k^T \mathbf{F}_M \mathcal{Y}_j. \quad (16)$$

4. Bit error rate (BER) analysis

The BER analysis of the MIMO SC-FDMA over Rayleigh fading channels in case of perfect CFO and ZF channel equalization is presented in this section. Several signal processing operations are applied to the received signals as in (5). These operations are removing the cyclic prefix, M -point FFT, sub-carrier de-mapping, frequency domain equalization (FDE) and CFO compensation, removing the training sequence, and N -point IFFT. By applying these operations successively, to get the k^{th} user received signal \mathbf{y}^k as in (16)

$$\mathbf{y}^k = \mathbf{d}^k + \mathbf{n}^k = \begin{bmatrix} \mathbf{y}_1^k \\ \vdots \\ \mathbf{y}_{N_r}^k \end{bmatrix} = \begin{bmatrix} \mathbf{d}_1^k \\ \vdots \\ \mathbf{d}_{N_r}^k \end{bmatrix} + \begin{bmatrix} \mathbf{F}_N^H & \cdots & 0 \\ \vdots & \ddots & \vdots \\ 0 & \cdots & \mathbf{F}_N^H \end{bmatrix} \begin{bmatrix} \mathbf{E}_{11}^k & \cdots & \mathbf{E}_{1N_r}^k \\ \vdots & \ddots & \vdots \\ \mathbf{E}_{N_r1}^k & \cdots & \mathbf{E}_{N_rN_r}^k \end{bmatrix} \begin{bmatrix} \mathbf{M}_k^T \mathbf{F}_M \mathbf{n}_1 \\ \vdots \\ \mathbf{M}_k^T \mathbf{F}_M \mathbf{n}_{N_r} \end{bmatrix}, \quad (17)$$

The complex Gaussian noise vectors are assumed to be $\mathbf{n}_i \sim \mathbb{C}\mathcal{N}(0; \sigma_{\eta}^2 \mathbf{I})$, $i = 1, 2, \dots, N_r$.

$$\mathbf{n}^k = \begin{bmatrix} \mathbf{F}_N^H & \cdots & 0 \\ \vdots & \ddots & \vdots \\ 0 & \cdots & \mathbf{F}_N^H \end{bmatrix} \begin{bmatrix} \mathbf{E}_{11}^k & \cdots & \mathbf{E}_{1N_r}^k \\ \vdots & \ddots & \vdots \\ \mathbf{E}_{N_r1}^k & \cdots & \mathbf{E}_{N_rN_r}^k \end{bmatrix} \begin{bmatrix} \mathbf{M}_k^T \mathbf{F}_M \mathbf{n}_1 \\ \vdots \\ \mathbf{M}_k^T \mathbf{F}_M \mathbf{n}_{N_r} \end{bmatrix}, \quad (18)$$

To calculate the variance of \mathbf{n}^k , the following step are carried out. The FFT, IFFT and subcarrier de-mapping operations do not affect the noise variance with using the isometric FFT matrix.

For the case of multiplying a diagonal matrix Λ of size $N \times N$ by a noise vector $\boldsymbol{\eta} \sim \mathbb{C}\mathcal{N}(0; \sigma_{\eta}^2 \mathbf{I})$. The resultant variance is given by

$$E((\Lambda \boldsymbol{\eta})(\Lambda \boldsymbol{\eta})^H) = E(\Lambda \boldsymbol{\eta} \boldsymbol{\eta}^H \Lambda^H) = \Lambda (\sigma_{\eta}^2 \mathbf{I}) \Lambda^H = \sigma_{\eta}^2 \Lambda \Lambda^H. \quad (19)$$

Thus, the average value of the variance in this case will be

$$\sigma_{\Lambda \boldsymbol{\eta}}^2 = \frac{\sigma_{\eta}^2}{N} \sum_{n=1}^N |\Lambda(n, n)|^2 = \beta \sigma_{\eta}^2. \quad (20)$$

Provided the above effects on the noise variance, it is clear that the complex Gaussian noise vectors $\mathbf{n}_i \sim \mathbb{C}\mathcal{N}(0; \sigma_{\eta}^2 \mathbf{I})$, $i = 1, 2, \dots, N_r$. Variances are affected by multiplication by diagonal matrices and additions during the equalization process as in (18). Thus, by using the relation (20), the variances of can be written as

$$\sigma_{\mathbf{n}^k}^2 = \sigma_{\eta}^2 \sum_{i=1}^{N_r} \beta_{ii}. \quad (21)$$

For a QPSK (as an example) modulated data symbol vector \mathbf{d}^k in (17) and a noise variance as in (21). The symbol error rate for proposed system can be written as

$$P_e = Q\left(\sqrt{\frac{E_s}{\sigma_{n^k}^2}}\right) \quad (22)$$

where E_s is the average symbol energy for QPSK case. $E_b = \frac{E_s}{2}$ is the average bit energy and $\sigma_{n^k}^2$ is the processed noise energy (variance). $Q(\cdot)$ is the Q-function which is defined as $Q(x) = \frac{1}{\sqrt{2\pi}} \int_x^\infty e^{-\frac{v^2}{2}} dv$.

5. Computational complexity

In this section, studying the computational complexity of the proposed MIMO single-carrier FDMA. Where it studies the number of complex multiplications. The complexity of proposed MIMO SC-FDMA system depends on N -FFT and M -IFFT in transmitter and N -IFFT, M -FFT, MMSE equalizer, and CFO estimator in receiver. As known the computational complexity of N -FFT operation is $\mathcal{O}N \log_2 N$. While the computational complexity of M -FFT operation is $\mathcal{O}M \log_2 M$. So the complexity for proposed MIMO SC-FDMA transmitter is $\mathcal{O}((\log_2 N + 2Q \log_2 Q)N)$ as $M = QN$. To calculate the computational complexity of MMSE equalizer in receiver, lets first know equalizer depends on multiplication of matrix and inversion of matrix which of size $2N \times 2N$. Where its complexity is $\mathcal{O}((2N)^3)$. From E_{ji}^k equalizer equation (5), it composed of four diagonal matrices multiplied by its conjugate transpose. The computational complexity for equalizer equation will be $\mathcal{O}(4N)$. By studying equation (6) it composed of four diagonal matrices of inversion of $2N$ of size 2×2 with complexity $\mathcal{O}(8N)$. Thus leads to the computational complexity of equalization process will be $\mathcal{O}(20N)$. Where the process of equalization composed of one inversion matrix and three matrix multiplications. Last part of receiver having complexity is CFO estimator. From equation (7) $P(m)$, the computational complexity is $2N^2$.

6. Simulation and results

The simulation parameters executed in this section are listed in Table 2. Different methods of CFO estimation sequences are

considered to illuminate effects of CFO. The considered methods are Schmidl and Cox method [14], Minn's Method [15] and Park's Method [16,17], CAZAC sequence [18–20], and the proposed CAZBAR sequence.

A. Timing Metric

Fig. 4 shows the timing metric by using different methods Schmidl and Cox, Park, Minn, and CAZAC sequence, and the proposed CAZBAR sequence.

As the Fig. 4 shows, schmidl has plateau which lead inaccurate starting point of frame around 50. Minn sequence shows several peaks around the starting point. Park methods gets sharp peak comparing with Minn at same starting point at 50. However, CAZAC method get the sharper starting point which is adjusted at 80. Now by comparing the proposed (CAZBAR) method with the CAZAC, the proposed method is adjusted at 55 to avoid overlapping with other methods. It shows sharper peak without ripples, lead to perfect CFO estimation.

B. Mean Square Error MSE

Fig. 5 illustrates the CFO estimation performance in terms of mean square error (MSE) versus SNR. The MSE is average squared difference between the estimated CFO values and the actual CFO value. It is clear from Fig. 5 that the proposed method has a smaller MSE and hence a more accurate CFO estimation than the other algorithms. As Schmidl & Cox. ends at 0.003646, while Minin, park, CAZAC, and proposed CAZBAR sequence end at 0.0002615, 0.0001752, 0.0006148, and 0.0001115 respectively.

Table 2 The simulation system parameters.

Parameter	Value or Type
Modulation	BPSK, QPSK, and 16 QAM
Cyclic Prefix	16 Samples
Output Block Size (M-IFFT)	256
Input Block Size (N-FFT)	128
Equalization Type	MMSE
Subcarrier Mapping Type	Localized & Interleaved
MIMO Size	2×2 and 4×4

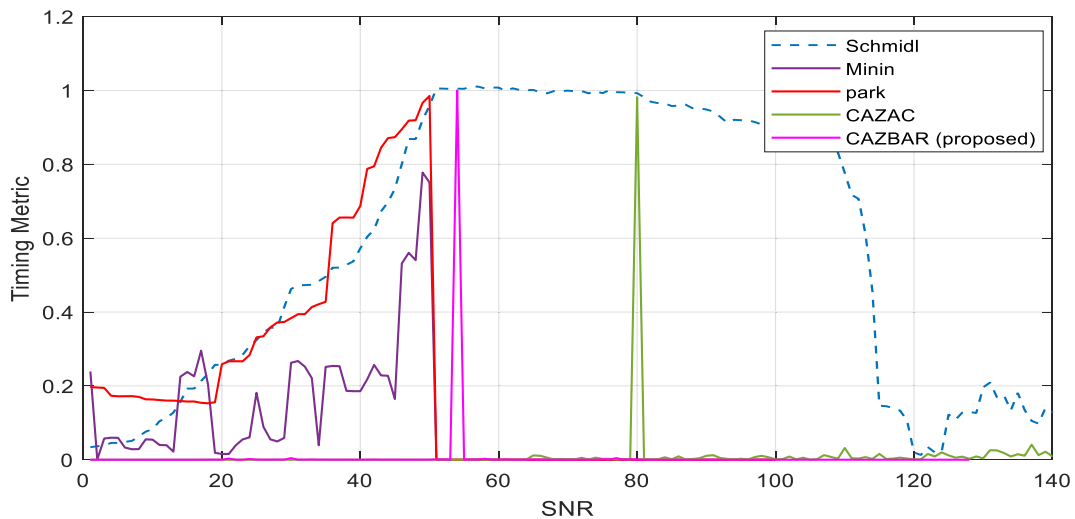


Fig. 4 Timing metric of OFDM system using Schmidl & Cox, Minn, Park, and CAZAC Methods, CAZBAR the Proposed Sequence.

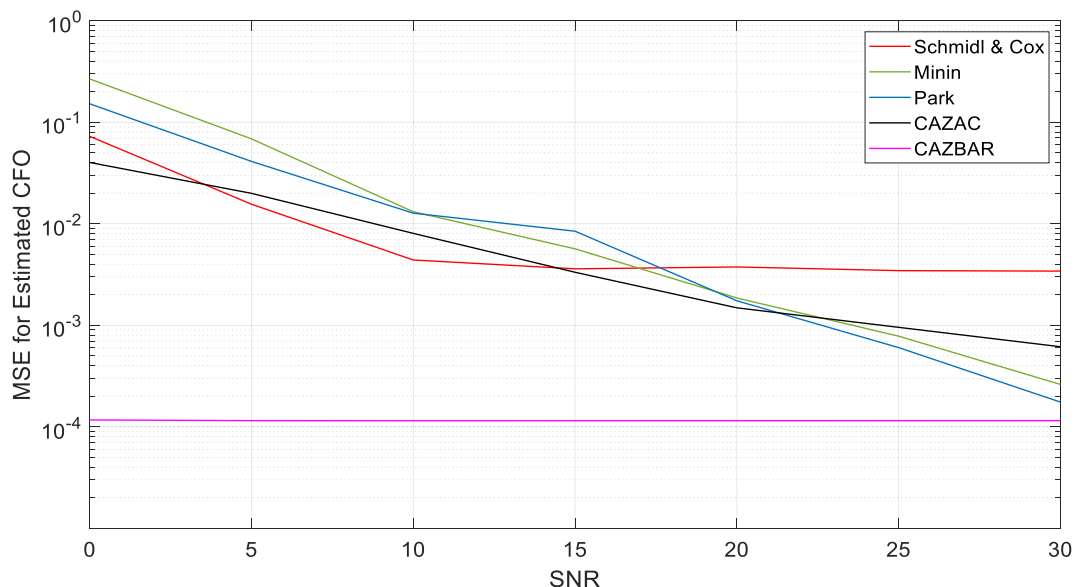


Fig 5 Mean Square Error (MSE) of estimated CFO for Schmidl & Cox., Minin, Park, CAZAC, and Proposed CAZBAR sequence.

B. Analytical BER Vs Simulated BER

Fig. 6 studies difference between analytical BER that results from previous equations (37) and Simulated BER. The system is applied on different modulation techniques as BPSK, QPSK, and 16 QAM. As shown the two curves are coincided together in case of zero forcing (ZF) equalization with perfect channel states information (CSI).

C. BER Performance

The proposed method MIMO- SC-FDMA depends on combining single-carrier FDMA (SC-FDMA) with multiple input multiple output (MIMO) and applying CFOs, then trying to estimate offset with the previous estimation methods as shown above. In the proposed MC-SC-FDMA, the modulation applied is BPSK. MMSE equalization technique are applied. The performance of bit error rate (BER) of proposed MIMO SC-FDMA system.

Fig. 7 proposed MIMO-SC-FDMA by applying 2×2 MIMO system over Rayleigh fading channel. Obviously Schmidl & Cox reach SNR 30 dB at $BER = 10^{-2}$. While, Minn and Park 25 dB, 22 dB respectively at $BER = 10^{-2}$. By CAZAC method BER performance improves to reach 19 dB at 10^{-2} . The proposed sequence CAZBAR with barker length $L = 2$, it gives better performance to reach 11 dB at 10^{-2} . The difference between the proposed sequence and CAZAC method is 8 dB.

Fig. 8 shows the comparison between the estimated and known CFO of the proposed MIMO-SC-FDMA. It applied on various modulation techniques as BPSK, QPSK, and 16-QAM. As shown in Fig. 8 the two curves look like each other. Which indicates the estimated curve of proposed MIMO-SC-FDMA shows good performance and cannot enhanced more than that.

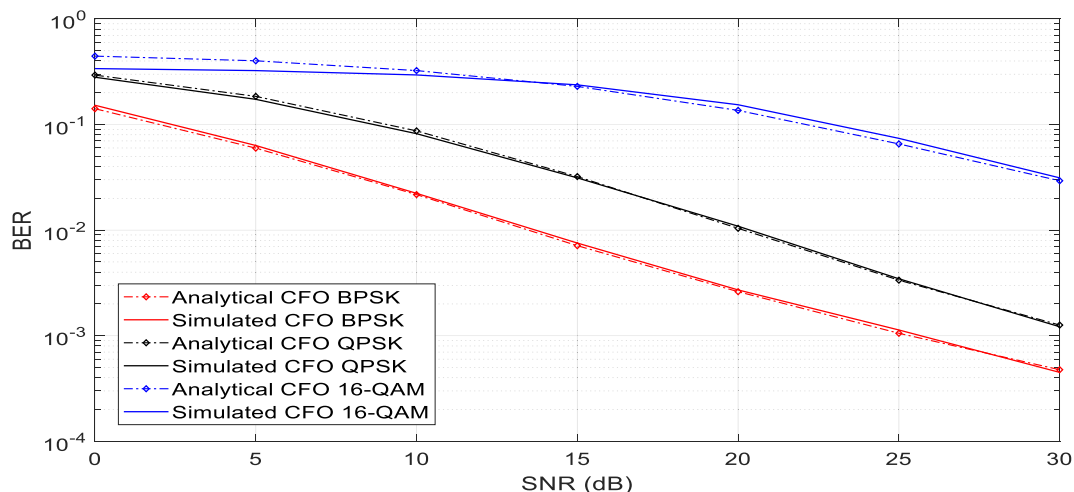


Fig. 6 Analytical BER Vs Simulated BER.

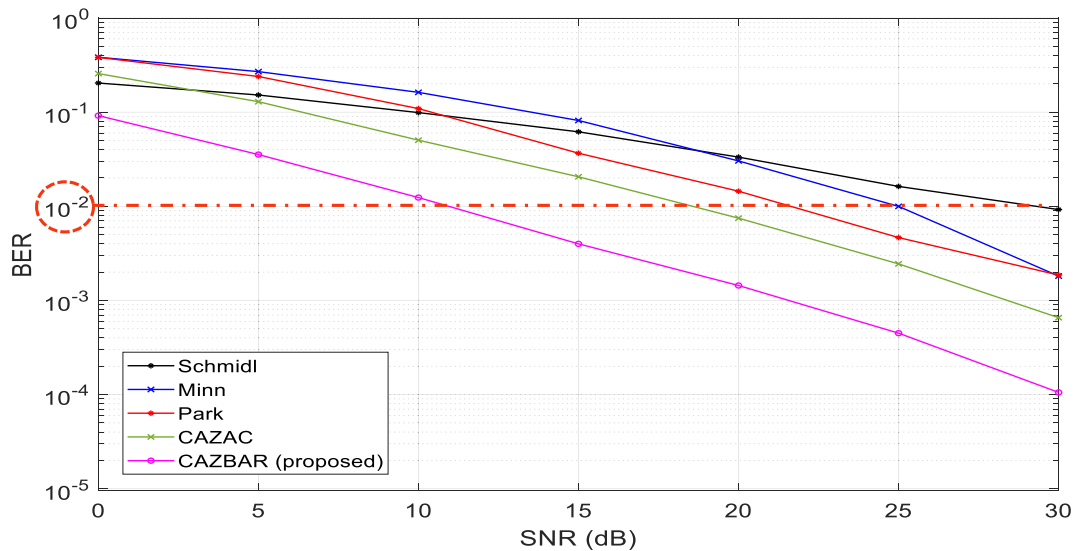


Fig.7 BER Curve of proposed 2x2 SC-FDMA system using different estimation methods: Schmidl, Minn, Park, CAZAC and Proposed Sequence.

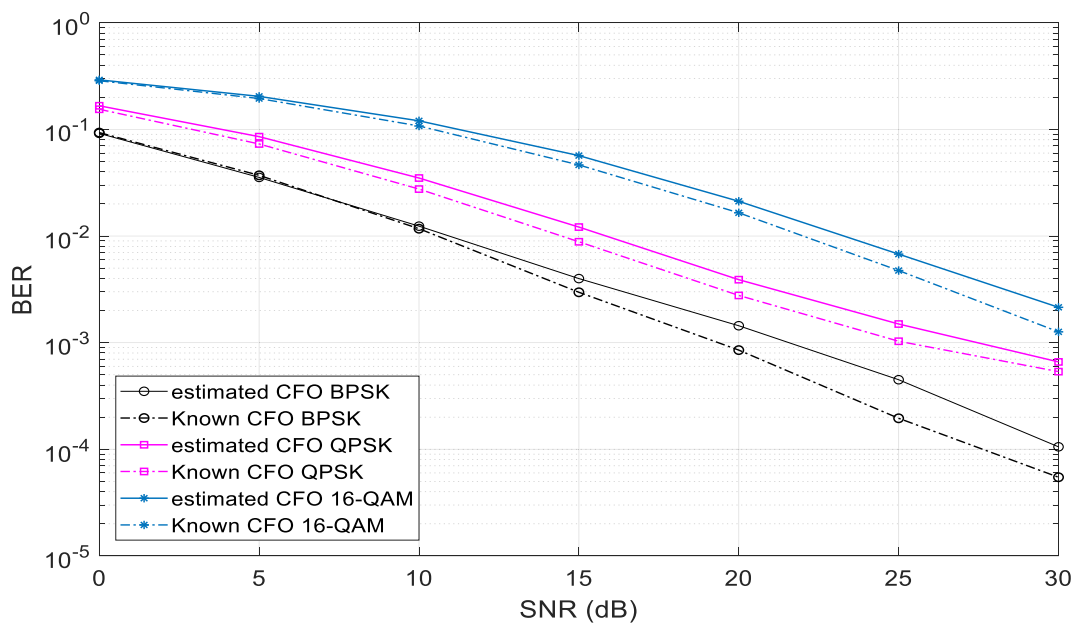


Fig. 8 Estimated CFO Vs Known CFO.

Fig. 9 the proposed MIMO-SC-FDMA by applying 4×4 MIMO system over Rayleigh fading channel. As shown Schmidl & Cox worst performance as cannot reach BER at 10^{-3} as previous. While Minn improves slightly to reach 23.5 dB, 20 dB respectively at $BER = 10^{-2}$. While in CAZAC method BER performance improves to 16.5 dB at 10^{-2} . Where the proposed sequence CAZBAR gives better performance comparing by previous methods to reach 7 dB at 10^{-2} . The difference between the proposed sequence and CAZAC method is 9.5 dB.

Fig. 10 shows the comparison between the estimated and known CFO of the proposed 4×4 MIMO-SC-FDMA. It applied on various modulation schemes as BPSK, QPSK, and 16- QAM. As seen in Fig. 10 the two curves are similar.

The estimated curve of proposed MIMO-SC-FDMA shows good performance and cannot improved further.

7. Conclusion

In this paper, novel preamble is used in MIMO SC-FDMA transceiver system. First study the performance of CAZBAR code. This code shows better autocorrelation especially with barker length $L = 2$. Paper is divided into two parts, first part study the formation of CAZBAR sequence, CFO estimation methods and to illustrate the accuracy of the CFO estimation of the previous methods by using the mean square error

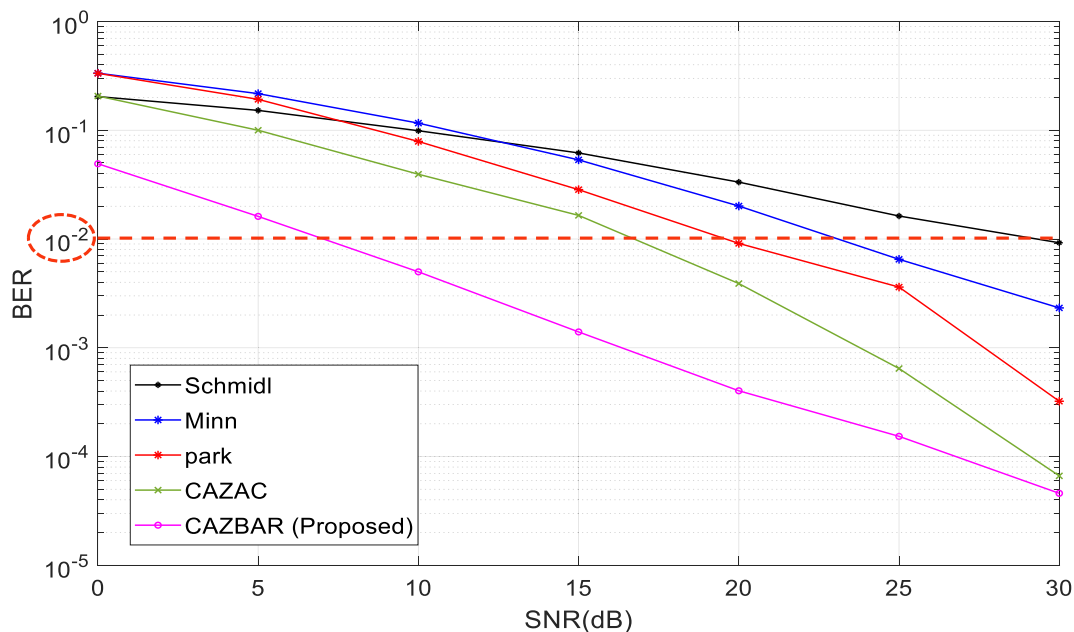


Fig. 9 BER Curves for 4x4 SC-FDMA system (BPSK) using Schmidl, Minn, Park, CAZAC and Proposed CAZBAR Sequence.

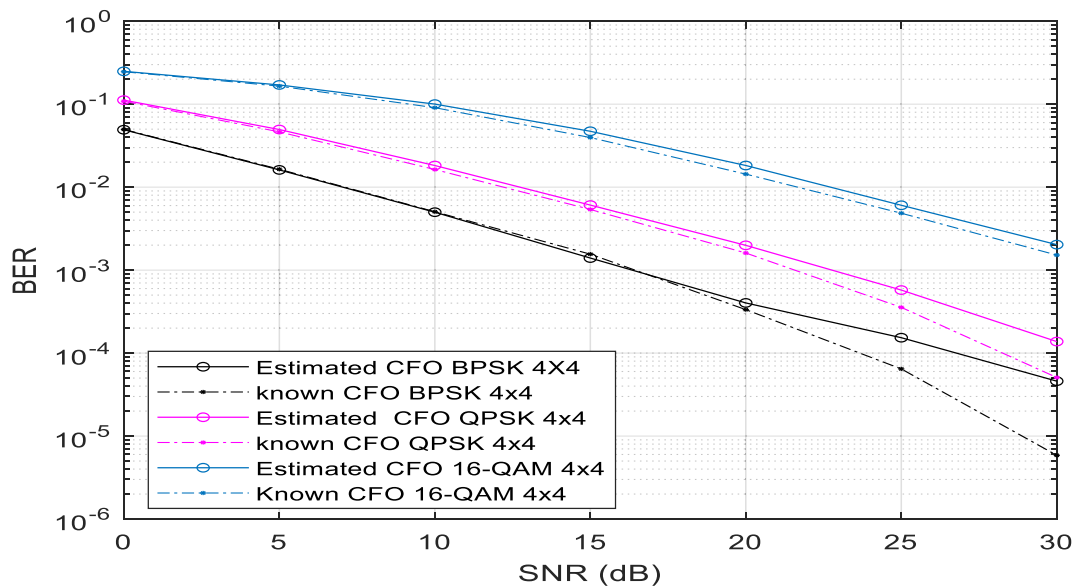


Fig. 10 Estimated CFO Vs Known CFO through proposed MIMO-SC-FDMA 4 x 4 system.

(MSE). Second part shows BER performance of proposed MIMO SC-FDMA by using proposed estimation and comparison with the other estimation methods. Simulation results show by using proposed estimated method got sharper timing metric without ripples. By applying CAZBAR sequence in MIMO SC-FDMA system 2 x 2 and 4x4, the bit error rate (BER) performance has improved significantly to reach 11 dB in 2 x 2 system and 7 dB in 4 x 4 system compared to other sequences. Also has a smaller MSE to reach 0.000115 at SNR = 30.

Declaration of Competing Interest

The authors declare that they have no known competing financial interests or personal relationships that could have appeared to influence the work reported in this paper.

Acknowledgement

None

References

- [1] M.M. Gul, S. Lee, X. Ma, PARAFAC-based frequency synchronization for SC-FDMA uplink transmissions, *EURASIP J. Adv. Signal Process.* 2014 (2014) 146.
- [2] S.A. Aburakhia, E.F. Badran, D.A.E. Mohamed, Linear companding transform for the reduction of peak-to-average power ratio of OFDM signals, *IEEE Trans. Broadcast.* 55 (1) (2009) 155–160.
- [3] S.A. Sulaiman, E.F. Badran, D.A. Mohamed, A comparison between clipping and μ -law companding schemes for the reduction of peak-to-average power ratio of OFDM, in: 2007 National Radio Science Conference, Cairo, Egypt, 2007, pp. 1–10.
- [4] E.F. Badran, A.M. El-Helw, A novel semi-blind selected mapping technique for PAPR reduction in OFDM, *IEEE Signal Process Lett.* 18 (9) (2011) 493–496.
- [5] A.I. Zaki, A.A. Hendy, W.K. Badawi, E.F. Badran, Joint PAPR reduction and sidelobe suppression in NC-OFDM based cognitive radio using wavelet packet and SC techniques, *Phys. Commun.* 35 (2019) 100695.
- [6] S. Kumar, S. Majhi, C. Yuen, Multi-user CFOs estimation for SC-FDMA system over frequency selective fading channels, *IEEE Access* 6 (2018) 43146–43156.
- [7] V. Dalakas, P.T. Mathiopoulos, F. Di Cecca, G. Gallinaro, A comparative study between SCFDMA and OFDMA schemes for satellite uplinks, *IEEE Trans. Broadcast.* 58 (3) (2012) 370–378, <https://doi.org/10.1109/TBC.2012.2193494>.
- [8] M. Alibakhshikenari, B.S. Virdee, M. Khalily, C.H. See, R. Abd-Alhameed, F. Falcone, T.A. Denidni, E. Limiti, High-gain on-chip antenna design on silicon layer with aperture excitation for terahertz applications, *IEEE Antennas Wirel. Propag. Lett.* 19 (9) (2020) 1576–1580, <https://doi.org/10.1109/LAWP.2020.3010865>.
- [9] M. Alibakhshikenari et al, A comprehensive survey on various decoupling mechanisms with focus on metamaterial and metasurface principles applicable to SAR and MIMO antenna systems, *IEEE Access* 8 (2020) 192965–193004.
- [10] E.F. Badran, A.Y. Alamri, M.A. Mokhtar, E.-S. El-Badawy, A space wavelet block codes MIMO SC-WDMA systems, *Phys. Commun.* 36 (2019) 100804, <https://doi.org/10.1016/j.phycom.2019.100804>.
- [11] E.F. Badran, DWT-based joint antenna selection for correlated MIMO channels, *J. Signal Image Video Process.* 3 (1) (2009) 35–45.
- [12] E.F. Badran, A.A. Bashir, A.I. Zaki, W.K. Badawi, Orthogonal codes-based dynamic spectrum access in cognitive radio networks, *China Commun.* 16 (12) (2019) 34–46, <https://doi.org/10.23919/JCC.2019.12.002>.
- [13] A.Y. Alamri, E.F. Badran, A space-frequency block codes MIMO single-carrier code-frequency division multiple access system, *AEU – Int. J. Electron. Commun.* 116 (2020) 153053, <https://doi.org/10.1016/j.aeue.2019.153053>.
- [14] T.M. Schmidl, D.C. Cox, Robust frequency and timing synchronization for OFDM, *IEEE Trans. Commun.* 45 (12) (1997) 1613–1621, <https://doi.org/10.1109/26.650240>.
- [15] H. Minn, M. Zeng, V.K. Bhargava, On timing offset estimation for OFDM systems, *IEEE Commun. Lett.* 4 (7) (2000) 242–244, <https://doi.org/10.1109/4234.852929>.
- [16] B. Park, H. Cheon, C. Kang, D. Hong, A novel timing estimation method for OFDM systems, *IEEE Commun. Lett.* 7 (5) (May 2003) 239–241, <https://doi.org/10.1109/LCOMM.2003.812181>.
- [17] B. Park, H. Cheon, C. Kang, D. Hong, A simple preamble for OFDM timing offset estimation 2 (2002) 729–732, <https://doi.org/10.1109/VETEFCF.2002.1040695>.
- [18] R. Heimiller, Phase shift pulse codes with good periodic correlation properties, *IRE Trans. Inf. Theory* 7 (4) (1961) 254–257, <https://doi.org/10.1109/TIT.1961.1057655>.
- [19] R. Frank, S. Zadoff, R. Heimiller, Phase shift pulse codes with good periodic correlation properties (Corresp.), *IRE Trans. Inf. Theory* 8 (6) (1962) 381–382, <https://doi.org/10.1109/TIT.1962.1057786>.
- [20] H. Asran, E.F. Badran, A.I. Zaki, Novel time and frequency synchronization techniques for OFDM Systems in double selective fading channel, *Wireless Pers Commun* 81 (1) (2015) 225–238.